International Journal of Engineering

Journal Homepage: www.ije.ir

Effect of Friction Stir Processing on Fusion Welded Joint of Al-5083

K. D. Tandel*, J. V. Menghani

Sardar Vallabhbhai National Institute of Technology, Surat, India

PAPER INFO

Paper history:
Received 07 April 2022
Received in revised form18 May 2022
Accepted 26 May 2022

Keywords:
Friction Stir Processing
Surface Modification
Autogenous TIG Welding
Grain Refinement

ABSTRACT

Tungsten Inert Gas Welding (TIG) is the most preferred joining process for aluminum alloys, but it produces weld joint having inferior mechanical property in comparison with base metal because of inherent limitations of the process. To improve the mechanical properties, the weld is post processed by friction stir processing (FSP) upto depth of 2mm. This paper presents the effect of performing FSP on autogenous TIG welded butt joint of Al-5083, 6mm thick plate. Mechanical and metallurgical properties of both processed and unprocessed autogenous TIG weld are compared. Characterisation techniques adopted to evaluate weld joint are tensile test, microhardness measurement, microstructural examinations and SEM analysis. Tensile strength of autogenous TIG weld joint is lowered by 6.5% compared to base metal because of presence of micro porosities in the weld metal. Friction stir processing produces the fine grain refined structure, marginally improves the tensile strength of the autogenous TIG weld joint by 2.7%. Microhardness of the autogenous TIG weld metal of the surface is raised from 163.6 HV to 298 HV after performing FSP. However, SEM images of fractured surface of friction stir processed specimen reveals fine dimpled structure which indicates that ductility of the weld joint remain unaffected after performing FSP on autogenous TIG weld joint.

doi: *10.5829/ije.2022.35.09c.09*

1. INTRODUCTION

Recent advancements in the field of marine, automobile, defence and aerospace propel the usage of light metals such as aluminum, titanium and magnesium against the conventional materials. 5xxx, 6xxx and 7xxx series of aluminum alloys possesses excellent mechanical and physical properties such as high strength to weight ratio, good corrosion resistance in extreme conditions, low density, good formability and high thermal conductivity. That is why they have been the prime choice for manufacturing various components used in interceptor boat structure, car frame and bodies, axles, shafts, air craft, missile, rocket and rocket launcher [1].

Tungsten Inert Gas Welding (TIG) has been the preferred fusion welding technique over Shielded Metal Arc Welding (SMAW), and Metal Inert Gas Welding (MIG) for manufacturing of aluminium alloy structures and components because of its ability to produce deeper penetration and cleaner weld joint [2]. As the aluminum alloys are having high heat conductivity, high thermal expansion coefficient, and inclination for refractory aluminium oxide (Al_2O_3) generation, fusion welding of aluminium alloys is challenging [3]. Furthermore, welding flaws associated with fusion welding of aluminum alloy such as porosity, low wetting, hot cracking, lack of fusion, residual stresses, and distortion are responsible for decrease in strength, and poor joint efficiency [4, 5]. However, the rising use of aluminium alloys in practically every industry is forcing researchers to create practicable and effective technologies to weld aluminium alloys without compromising their mechanical, chemical, or metallurgical properties, which are required for longer service life.

Being a green technology by nature, friction based welding and surface processing techniques have been very popular since last two decades and best suited for welding and processing of aluminum alloys as it does not melt the base metal [6]. The Welding Institute (TWI) in the UK first invented and patented the novel Friction Stir Welding (FSW) process in the year 1991. The process involves generation of frictional heat using non-consumable spinning tool with a probe/pin and a collar plunged in to the metals to be joined and traverse along

*Corresponding Author Email: kdtandel.gecd@gmail.com (K. D. Tandel)

Please cite this article as: K. D. Tandel, J. V. Menghani, Effect of Friction Stir Processing on Fusion Welded Joint of Al-5083, ***International Journal of Engineering, Transactions C: Aspects***, Vol. 35, No. 09, (2022) 1735-1743

the intended welding path [7]. The material around the tool probe softens due to frictional heating generated due to rubbing action of tool and base metal. Extreme plastic deformation and plastic material flow all around the tool probe are caused by the combined impact of tool rotational and transverse movement. The churning of two base metals in a plastic state around the tool produces a permanent weld joint upon cooling to room temperature [8]. FSW-produced joint possesses superior mechanical property compared to fusion welded joints of aluminum alloys because in FSW process, weld metal experiences an excessive plastic deformation at elevated temperature, breaks dendritic coarse grain structure, and produces fine and equiaxed recrystallized structure [6]. However, the mechanical characteristics of the weld joint is greately affected by the FSW operating parameters and tool geometry [9]. As the heat produced by friction is directly proportional to the tool rotation speed, the tensile strength increases as tool rotation speed increases and decreases as tool traverse feed increases [10].

A newer welding approach of surface modification by Friction Stir Processing (FSP) has been successfully demonstrated by many researchers. FSP is a novel varient of FSW, introduced by Mishra et al. [11], having the same working principle as that of FSW, in that a rotating tool is inserted into the material surface up to a specific targeted depth and travelled along the required path to cover the material's intended surface area with the purpose of modifying the microstructure and consequently changing the material's surface mechanical characteristics [12]. Later on fabrication of composite of SiC reinforcement in the Al-5083 metal matrix was successfully demonstrated by Mishra et al. [11]. The experimental results show substantial increase in the hardness of the FSPed segment in comparison with the base metal. The SiC particles were well dispersed throughout the aluminium matrix, demonstrating good bonding with the aluminium alloy substrate. Factors like tool geometry, number of FSP passes, FSP operating parameters (tool rpm and travel speed), and the type and volume fraction of metal matrix composite fabrication are responsible for the desired change in surface properties [13]. Wang et al. had successfully fabricated SiCp reinforced Al metal matrix composites (MMCs) up to the depth of 100 μm using FSP technique. Increase in top surface micro hardness value of about 10% compared to base metal was reported by addition of SiCp (1.5%) to aluminum matrix [14]. Kaushik and Singhal [15] studied effect of FSP on microstructural and mechanical behavior of friction stir welded aluminum alloy 6063 matrix reinforced with 7 wt% SiC particles. Uniform distribution of SiC particles in Al-6063 matrix was observed after FSP. Significant improvement in wear resistance property of Al-TiC composite using FSP was reported by Akinlabi et al. [16]. Wear resistance property was found to be influenced by tool rotation speed and processing feed rate. Multipass FSP was used by Bauri et al. [17] to homogenise the TiC particle dispersed in an aluminium matrix. After each FSP pass, the grain size was refined which significantly improved mechanical property without compromising ductility. Sharma et al. [18] had employed variety of FSP methods including varying process parameters, dual-tool processing and tool offset overlapping to produce SiC reinforced AA5083 alloy surface. Success of the FSP as a surface modification technique has been a driving force for many researchers to execute the same on welded surface. To enhance fatigue charecteristics of the weld joint, Costa et al. [19] and Borrego et al. [20] had performed FSP on the toe of the T-joint and butt joint of Al-5083 welded by Metal Intert Gas (MIG) welding process respectively. Xu and Bao [21] claimed that mechanical properties of weld joint of AZ31 magnesium alloy performed by TIG welding process was improved after performing rapid cooled FSP on it. Friction Stir Processed (FSPed) TIG and Friction Stir Welded joints were tested by Mabuwa and Msomi [22]. In the work, full depth FSP showed significant improvement in tensile strength while hardness was marninally affected [22]. Al-5052 alloy weldment produced by TIG welding process, which was post processed by a newer method called friction stir vibration processing (FSVP) showed greater grain refinement in the stir zone which leads to increase in tensile strength by 17% and improvement in ductility by 33% compared to unprocessed TIG weld joint [23]. Mehdi and Mishra [24] studied effect of FSP on mechanical property and heat transfer of TIG weld joint of dissimilar aluminum alloy AA-6061 and AA-7075. The calculated maximum temperature using ANSYS software was around 515°C tool rotation speed of 1600 RPM whereas maximum rate of heat flux was calculated about 5.33 x 10^6 W/m^2 observed at tool rotation speed of 1600 RPM.

In the present investigation, Al-5083 plate of 6mm thickness was butt welded by TIG welding technique without addition of filler wire (autogenous welding). The weld was then friction stir processed (FSPed) with a solid tool having a pin. The processing was achieved upto depth of 2mm on both sides. Characterisation of the weld joint produced was performed by macro observation, micro examination, tensile testing, and microhardness mapping. The nature of weld failure was investigated via fractographic examinations using scanning electron microscope (SEM). As per the reviewd literature, FSP upto depth of 2mm on both sides of autogenous TIG weld of Al-5083 is not observed. The present work is a step towards it.

2. MATERIALS AND METHODS

2. 1. Base Metal The base metal in this experiment was Al-5083, a 6mm thick plate. Aluminum alloy 5083 is an Al-Mg alloy which has the highest strength amongst

TABLE 1. Chemical composition of Al-5083

Mg	Mn	Fe	Si	Cr	Cu	Zn	Al
5	0.57	0.35	0.15	0.05	0.05	0.02	Rest

TABLE 2. Mechanical Properties of Al-5083

Property	Value
Tensile Yield Strength	228 MPa
Ultimate Tensile Strength	317 MPa
Elongation at Break	16%
Hardness	85 BHN

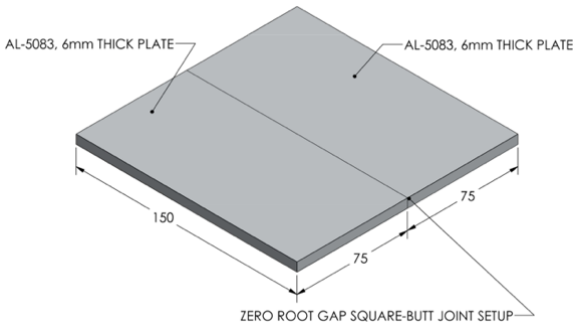

Figure 1. Weld setup for autogenous TIG welding

non-heat treatable alloys as well as it possesses excellent corrosion resistance in salt water which make it an ideal choice for chemical industry and marine applications [2]. According to ASTM B209/B928M, the chemical composition and typical mechanical properties of Al-5083 are presented in Table 1. Mechanical properties of Al-5083 collected from ASM data sheet is summarized in Table 2. Using a cutting wheel, the plate was cut into pieces of 150mm x 75mm. The plate's edges were flat ground to create a zero rootgap, Square-butt joint configuration for the autogenous TIG welding process is shown in Figure 1.

2. 2. Autogenous TIG Welding Aluminium-Mg alloy with Mg in the range of 1 to 2.5 percent may be prone to hot cracking if welded without filler wire or with a filler wire having matching chemical composition with base metal. To avoid hot cracking while welding of Al-Mg alloy, filler metal having Mg content greater than 3.5% is used [25]. Autogenous TIG welding arrangements are illustrated in Figure 1. The Lincoln Electric made Aspect-300 TIG welding equipment was used to execute TIG welding on square-butt joint. To accomplish a full penetration joint, single pass on each sides was deposited by TIG welding. Argon (99.998% purity) was used as the shielding gas, and a 3mm diameter Thoriated Tungsten rod was used as electrode. The electrode tip had a blunt conical form. The pointed tungsten electrode tip deteriorates quickly, causing the arc to wander during AC welding, resulting in a welding defect. The arc becomes steady when using a blunt electrode tip. Welding parameters to achieve full penetration joint by autogenous TIG welding process are 150 *amp* current, 15-16 *V* volatage, 120-130 *mm/min* travelspeed and 13-14 *lpm* shielding gas flow rate.

2. 3. Friction Stir Processing Autogenous TIG welded plate was friction stir processed (FSPed) on both side upto a depth of 2mm from the top surface by using a tool having a pin. Tool used in FSP is shown in Figure 2. Pin geometry was cylindrical and having a height of 2 mm. FSP was performed on Batiboi made milling machine. Figure 3 shows setup of FSP on milling machine. For FSP of TIG welded plate, different combination of tool rotation speed (500, 710, 1000 and 1400 rpm) and tool travel speed (40, 56 and 80 mm/min) are used. FSP parameters used for processing of TIG weld is shown in Table 3.

2. 4. Metallurgical and Mechanical Examination Macro examination of the TIG weld and FSPed sample was performed to ensure absence of macro flaws such as tunnel, pin hole, undercut, and porosity. Microstructural examination was performed using Carl Zeiss, Jena, Model-EPY Type-2 optical microscope. Specimen for micro examination was taken across the weld in order to

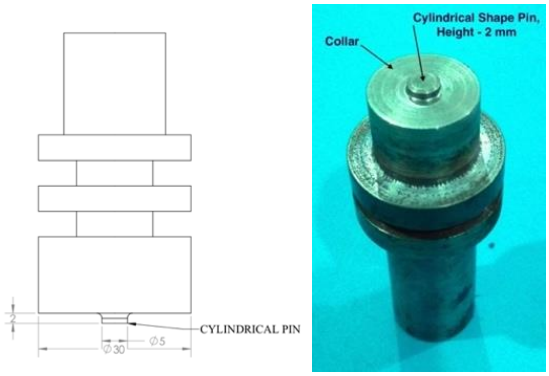

Figure 2. FSP Tool Having Cylindrical Pin Profile

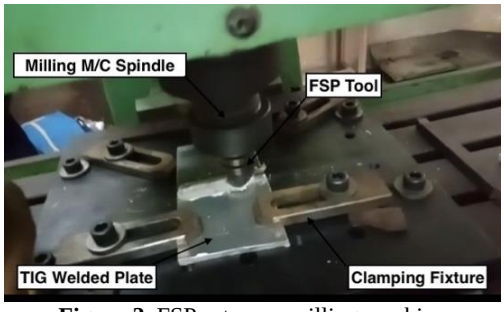

Figure 3. FSP setup on milling machine

TABLE 3. FSP Parameters and Tensile strength of autogenous TIG + FSP plate

Sample ID	Tool Rotation (RPM)	Feed Rate (mm/min)	Tensile Strength (MPa)	% Elongation	Remark
B1	-	-	298.3	22	Unaffected Base Metal
T2	-	-	278.5	20	Autogenous TIG Weld
TF13	500	40	286.1	22	-
TF14	500	56	279.7	22	-
TF15	500	80	-	-	Tunnel defect
TF3	710	40	273.1	20	-
TF2	710	56	173.3	8	Tunnel defect
TF8	710	80	268.7	16	Tunnel defect
TF6	1000	40	207.6	12	-
TF9	1000	56	195.1	10	-
TF7	1000	80	154.6	6	Tunnel defect
TF10	1400	40	196	10	-
TF11	1400	56	177.7	10	Tunnel defect
TF12	1400	80	-	-	Tunnel defect

observe base metal, heat affected zone (HAZ), thermo mechanically affected zone (TMAZ), stir zone (SZ), and weld metal microstructure. Etchant used for macro and micro examinations was Keller's reagent composed of 192ml distilled water, 5ml nitric acid, 3ml hydrochloric acid, 2ml hydrofluoric acid. Grain size (diameter) was digitally measured using ImageJ software.

Tensile test samples were collected from welded plate as well as unaffected base metal. Dimensions of the samples were kept as per ASTM B557. Dimensions of a sub-size flat tensile specimen is illustrated in Figure 4. Tensile test samples were sectioned across the weld axis. Tensile test was performed on a computerised tensometer, having 2T loading capacity. Test was performed at the speed of 10 mm/min. Change in hardness due to autogenous TIG welding and FSP was evaluated.

Microhardness was measured across the weld in FSPed and autogenous TIG weld region using a dimond indentor. Load applied during the test was 200gm for 20 second dwell time. The indentations were evaluated microscopically at the 100X magnification. Microhardness values were plotted against distance from weld center for all test specimens. Fracture surface of tensile test specimens were examined using Hitachi Made, Model - S-3400N scanning electron microscope at 1000X magnification. Fractured surface topography of tesile test specimens of autogenous TIG and FSPed specimens were throughly examined to understand the nature of failure.

3. RESULT AND DISCUSSION

3. 1. Macro and Micro Examination

Photographs shown in Figure 5 illustrates the as-welded appearance of autogenous TIG weld and FSPed TIG weld samples. Autogenous TIG welded plate using welding current of 150 *amp* and travel speed of 120 *mm/min*, displayed excellent bead finish in as welded condition, which does not demand for any post processing treatment. Furthermore, the surface macro flaws such as pin holes and undercut were also not observed on the weld surface (Figure 5(a)). Surface finish of FSPed plate was also good and no sign of tunnel defect was seen in the stir zone (SZ) (Figure 5(b)). Specimen shown in Figure 5(b) was FSPed at tool rotation and feed rate of 500 rpm and 40 mm/min, respectively. Autogenous TIG welded plate which was FSPed at higher feed rate (56 mm/min and 80 mm/min) showed tunnel defect as depicted in Figure 6. At faster feed rate material flow is insufficient to fill the void created by movement of FSP tool leads to tunnel defect in the SZ [28]. Autogenous TIG weld cross-

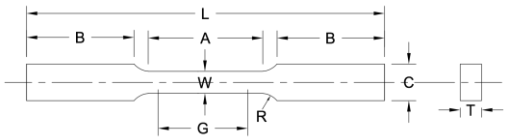

Nomenclature	Dimension in mm
Gauge length, G	25.00 ± 0.10
Width, W	6.01 ± 0.05
Thickness, T	Thickness of material (6mm)
Radius of fillet, R	6
Overall Length, L	100
Length of reduced section, A	32
Length of grip section, B	30
Width of Grip Section, C	10

Figure 4. Tensile Test Specimen Details as per ASTM B557

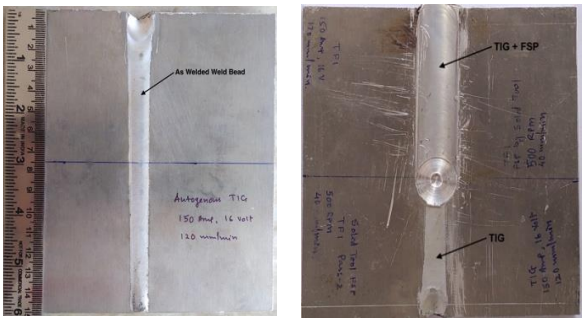

(a) (b)

Figure 5. As welded appearance of (a) Autogenous TIG welded plate, (b) TIG + FSP plate

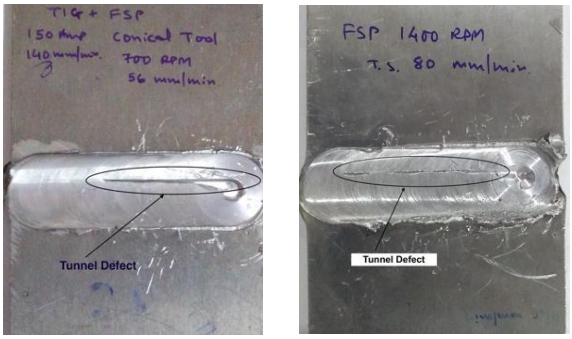

Figure 6. Tunnel Defect in FSP at Higher Travel Speed

According to the microstructural observation of autogenous TIG welded specimen, the weld and near vicinity regions are free from welding defects like void, crack and lack of fusion. However, small amount of micropores were observed in the weld region (Figure 7(b)). Elongated and distorted grains in the aluminum solid solution are observed in the microstructure of unaffected base metal mainly due to cold plate rolling (Figure 7 (d)). Weld metal microstructure reveals fine grain columnar structure (average grain size 22 μm) in aluminum solid solution. This is attributed to instant heating and cooling experienced by weld metal in welding process (Figure 7b). The HAZ, on the other hand, does not exhibit columnar grain structure but shows coarse grain and recrystallized structure (average grain size 35 μm) in aluminum solid solution as shown in Figure 7(c). The main reason behind grain coarsening in HAZ region is the welding heat input. Microstructural examination of FSPed specimen shows significant improvement in weld microstructure and will leads to enhanced mechanical property. Figure 8 shows microstructures of various zones of TIG + friction stir processed weld. Microstructure of stir zone depicts that coarse grained structure produced by autogenous TIG weld is well refined due to vigourous stirring effect produced by friction stir processing tool. Although temperature in the SZ is lower than the base metal's melting point but it is high enough to promote recrystallisation and produce fine grain equiaxed structure (average grain size 4.6 μm) in the SZ of FSPed region. Micro-pores present in autogenous TIG weld structure disappears from the stir zone of FSPed weldment due to stirring effect produced by FSP tool, which results in better mechanical property (Figure 8(b)). Microstructure of TMAZ reveals coarse grain dendritic structure (average grain size 30 μm) as shown in Figure 8(c). Microstructure of unprocessed TIG weld + FSP specimen shows coarser grain structure compared to autogenous TIG weld specimen without FSP as shown in Figure 8(d) (average grain size 57 μm). Heat input from the friction stir processing method is the reason behind grain coarsening.

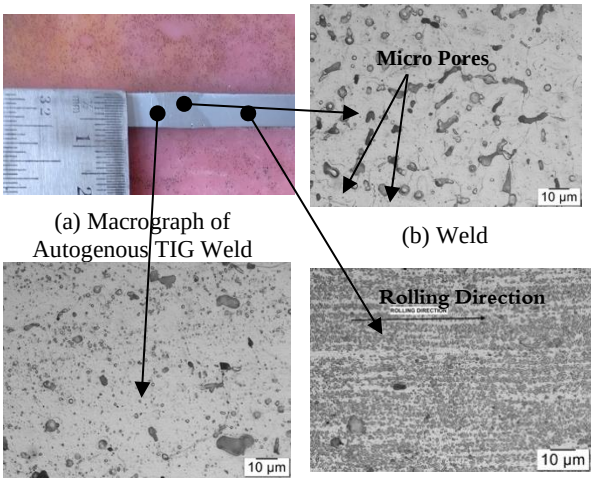

(a) Macrograph of Autogenous TIG Weld (b) Weld

(c) HAZ (d) Unaffected Base Metal

Figure 7. Macrograph and Microstructure of Autogenous TIG Weld at Different Locations: (a) Macrograph of Autogenous TIG Weld; (b) Weld (c) HAZ; (d) Base Metal, Magnification 500x

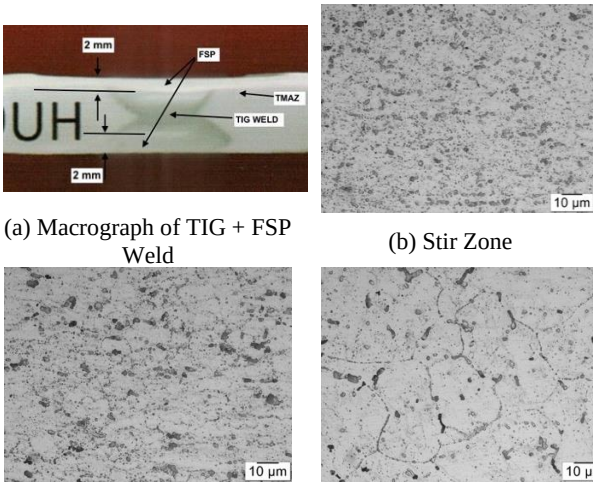

(a) Macrograph of TIG + FSP Weld (b) Stir Zone

(c) TMAZ (d) Unprocessed TIG Weld

Figure 8. Macrograph and Microstructure of Autogenous TIG + FSP Weld at Different Locations: (a) Macrograph of TIG + FSP Weld; (b) Stir Zone; (c) TMAZ; (d) Unprocessed TIG Weld, Magnification 500x

3. 2. Tensile Test Tensile strength and % elongation values of FSPed weld specimens are compiled in Table 3. Ultimate tesile strength values of unaffected parent metal and unprocessed autogenous TIG weld were also derived for comparison by performing tensile test. Figure 9 shows comparison of stress vs strain curve of parent metal, autogenous TIG welded plate (Sample T2, corresponding to maximum tensile strength among all autogenous TIG welded plates) and autogenous TIG + FSP plate (Sample TF13). Ultimate tensile strength of base metal (Sample B1), autogenous TIG (Sample T2) weld and TIG + FSP weld (Sample ID TF13) were found to be 298.3 MPa, 286.1 MPa and 278.5 MPa, respectively. It was observed that UTS of all the processed and unprocessed welded specimens were lower than UTS of unaffected base metal. This is because of the adverse effect of welding heat input on microstructure of Al-5083 alloy [26]. In addition to that, Al-5083 is a work hardened alloy possessing an unequiaxed grain structure in which grains are elongated in line with the direction of rolling as shown in Figure 7(d). During performing autogenous TIG welding process, due to welding heat input, effect of work hardening is destroyed, that leads to weakening of mechanical properties. During subsequent application of FSP on TIG weld recrystallisation reformed the microstructure resulting in improved mechanical properties [27]. Specimens processed at 80 mm/min feed rate (TF15, TF12) show full length tunnel defect hence tensile test can not be performed. Specimen processed at 500 rpm tool rotation speed and 40 mm/min feed rate (TF13) showed maximum ultimate tensile strength of 286.1 MPa and % elongation of 22% among all specimens processed at different tool rotation speed and feed rate. FSP displays marginal increase in tensile strength of around 2.7% compared to tensile strength of autogenous TIG welded specimen (278.5 MPa). This rise in the tensile strength is because of grain refinement and elimination of defects like micro porosity from the FSP region. However, all the welded specimens (autogenous TIG weld and autogenous TIG + FSP) display lower tensile strength as compared to parent metal. This is primarily due to reduction in strain hardening effect due to heat input given to the base metal during fusion welding and FSP [29].

3. 3. Microhardness Measurement Trend of microhardness variation across the weld for autogenous TIG and autogenous TIG followed by FSP samples are depicted in Figure 10. The weld zone of an autogenous

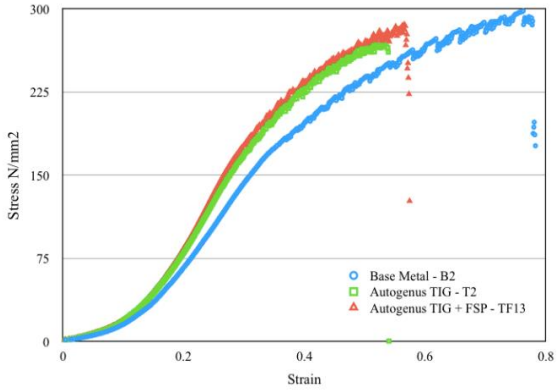

Figure 9. Tensile test curves for base metal, autogenous TIG (T2), and autogenous TIG+FSP (TF13)

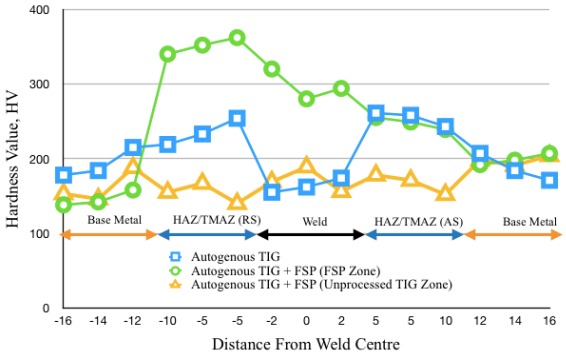

Figure 10. Microhardness profile across the weld

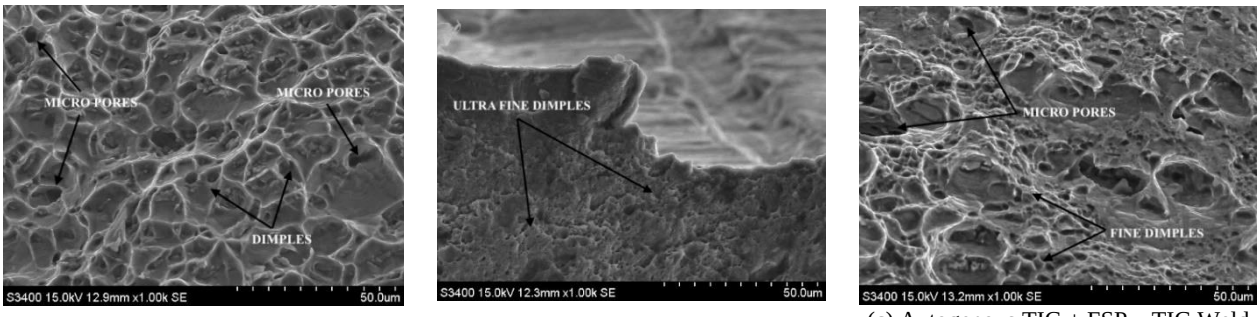

(a) Autogenous TIG Weld (b) Autogenous TIG + FSP – Stir Zone (c) Autogenous TIG + FSP – TIG Weld Center

Figure 11. SEM fractrograph of: (a) Autogenous TIG Weld; (b) Autogenous TIG + FSP - SZ, (c) Autogenous TIG + FSP – TIG Weld Center; Magnification 1000x

TIG welded specimen has a lower microhardness value than the base metal and HAZ/TMAZ. This could be due to re-precipitation of the β-phase Mg_2Al_3 during welding [30]. Because Al-5083 is a non-heat treatable alloy, lowering of hardness value as a result of welding heat input is not expected as plastic deformation is the primary hardening mechanism in this alloy [20]. Notable rise in hardness is reported in the SZ of FSP compared to autogenous TIG weld hardness. FSP causes excessive plastic deformation and promots well refined grain structure in the SZ. Also, Compressive stresses produced in the SZ during FSP minimizes the presence of micro-pores in the SZ leading to the increase in hardness in the SZ of FSP [15]. Microhardness of unprocessed TIG weld of FSPed specimen is almost unchanged in weld zone whereas HAZ microhardness is reduced due to added heat input during FSP [31]. Decrease in TMAZ hardness value away from the weld center towards advancing side is observed for TIG+FSP specimen. In FSP, the advancing side is the point at which a solid material begins to transform into a semi-solid phase and swirls about a tool pin which is inserted into the material. In the retreating side, the semi-solid phase retreated and cooled. As a result, during the FSW process, the advancing side, which has a more solid state nature at any point in time/location than the retreating side, should generate more frictional stresses, which generates more heat and elevates the peak temperature. This is attributed to the lower hardness value in the advancing side of FSP [11, 32].

3. 4 SEM Fractoscopy Scanning Electron Microscopy (SEM) was performed on the broken surface of tensile test samples of autogenous TIG and autogenous TIG + FSP weldment to analyse the nature of failure. The fractographs shown in Figure 11 reveals network of dimples in both specimens which indicates ductile failure. However, dimples observed in autogenous TIG + FSP weldment are much finer than that observed in autogenous TIG weld specimen. This is again due to the fact that FSP produces better refined structure compared to as welded autogenous TIG weld. Traces of micro porosities are also observed in SEM fractograph of autogenous TIG weld as shown in Figure 11(a). SEM fractograph of unprocessed TIG weld region of FSPed specimen shown in Figure 11(c) confirms the presence of micro-porosities and voids in the matrix of finer dimples compared to autogenous TIG weld specimen without FSP.

4. CONCLUSION

Friction Stir Processing (FSP) was performed on autogenous TIG weld surface to achieve structural modification and thus improving mechanical property of the weld joint. Conclusions derived from the present experimental work are as follows:

Full fusion butt weld joint of 6mm thickness is achieved through autogenous TIG welding process. Weld joint produced by autogenous TIG welding process exhibit lower tensile strength compared to base metal by 6.5%. The existence of micro-porosities in the TIG weld metal contributes to the decrease in weld joint's tensile strength.

Marginally increase (2.7%) in the tensile strength of autogenous TIG weld joint is observed after performing FSP on it. The grain refinement achieved by the FSP process is the reason behind improved tensile strength. Microhardness of autogenous TIG weld metal and HAZ region is substantially increased due to friction stir processing method. Percentage elongation value indicate that weld joint possesses good ductility in both autogenous TIG weld (20% elongation) and friction stir processed TIG weld (22% elongation). The SEM images of fractured surface of all tensile test specimens show series of dimple structure having different degree of fineness. Out of which, the FSPed specimen shows the most fine dimple structure.

Weldment which are friction stir processed at higher feed rates (56 mm/min and 80 mm/min) produces tunnel defect in the SZ due to insufficient heat input resulting in limited metal flow in the SZ.

Macroscopic and microstructural examination confirms that FSP can be used as weld joint surface modification technique. Churning and reheating of weld metal in the SZ during FSP causes grain refinement and recrystallisation leads to notable improvement in the weldment's surface characteristics.

5. REFERENCES

1. Miller, W. S., Zhuang, L., Bottema, J., Wittebrood, A., De Smet, P., Haszler, A. and Vieregge, A., "Recent development in aluminium alloys for the automotive industry", ***Materials Science and Engineering: A***, Vol. 280, No. 1, (2000), 37-49, doi: 10.1016/S0921-5093(99)00653-X.
2. Mabuwa, S. and Msomi, V., "Effect of Friction Stir Processing on Gas Tungsten Arc-Welded and Friction Stir-Welded 5083-H111 Aluminium Alloy Joints", ***Advances in Materials Science and Engineering***, Vol. 2019, (2019), 1-14, doi: 10.1155/2019/3510236.
3. Doshi, S., Gohil, A., Mehta, N. And Vaghasiya, S. "Challenges in Fusion Welding of Al alloy for Body in White", ***Materials Today: Proceedings***, Vol. 5, No. 2, Part 1, (2018), 6370-6375, doi: 10.1016/j.matpr.2017.12.247.
4. Ardika, R.D., Triyono, T. and Muhayat, N., "A review porosity in aluminum welding", ***Procedia Structural Integrity***, Vol. 33, (2021), 171-180, doi.org/10.1016/j.prostr.2021.10.021.
5. Mathers, G., "The welding of aluminium and its alloys", 1st ed. Woodhead Publishing Limited, 2002.
6. Wang, X., Wang, K., Shen, Y. and Hu, K. "Comparison of fatigue property between friction stir and TIG welds", ***Journal of***

University of Science and Technology Beijing, Mineral, Metallurgy, Material, Vol. 15, No. 3, (2008), 280-284, doi: 10.1016/S1005-8850(08)60053-5

7. Thomas, W. M., and R. E. Dolby. "Friction stir welding developments", Proceedings of the sixth international trends in welding research, (2003), 203-211.
8. Mishra, R. S., and Ma, Z. Y., "Friction stir welding and processing", ***Materials Science and Engineering: R: Reports***, Vol. 50, No. 1, (2005), 1-78, doi: 10.1016/j.mser.2005.07.001.
9. Fabregas Villegas, J., Martínez Guarín, A. and Unfried-Silgado, J., "A Coupled Rigid-viscoplastic Numerical Modeling for Evaluating Effects of Shoulder Geometry on Friction Stir-welded Aluminum Alloys", ***International Journal of Engineering Transactions B: Applications***, Vol. 32, No. 2, (2019), 313-321, doi: 10.5829/ije.2019.32.02b.17
10. Singh, R., Rizvi, S. A. and Tewari, S. P., "Effect of Friction Stir Welding on the Tensile Properties of AA6063 under Different Conditions", ***International Journal of Engineering Transactions A: Basics***, Vol. 30, No. 4, (2017), 597-603, doi: 10.5829/idosi.ije.2017.30.04a.19.
11. R. S. Mishra, Z. Y. Ma, and I. Charit, "Friction stir processing: a novel technique for fabrication of surface composite", ***Materials Science and Engineering: A***, Vol. 341, No. 1, (2003), 307-310, doi: 10.1016/S0921-5093(02)00199-5.
12. Su, J. Q., Nelson, T. W., and Sterling, C. J., "Microstructure evolution during FSW/FSP of high strength aluminum alloys", ***Materials Science and Engineering: A***, Vol. 405, No. 1, (2005), 277-286, doi: 10.1016/j.msea.2005.06.009.
13. Rao, D. S. and Ramanaiah, N., "Evaluation of Wear and Corrosion Properties of AA6061/TiB2 Composites Produced by FSP Technique", ***Journal of Minerals and Materials Characterization and Engineering***, Vol. 5, No. 6, (2017), 353-361, doi:10.4236/jmmce.2017.56029.
14. Wang, W., Shi, Q.Y., Liu, P., Li, H.K. and Li, T., "A novel way to produce bulk SiCp reinforced aluminum metal matrix composites by friction stir processing", ***Journal of Materials Processing Technology***, Vol. 209, No. 4, (2009), 2099-2103, doi: 10.1016/j.jmatprotec.2008.05.001.
15. Kaushik, N. and Singhal, S., "Experimental Investigations on Microstructural and Mechanical Behavior of Friction Stir Welded Aluminum Matrix Composite", ***International Journal of Engineering Transactions A: Basics***, Vol. 32, No. 1, (2019), 162-170, doi: 10.5829/ije.2019.32.01a.21
16. Akinlabi, E.T., Mahamood, R.M., Akinlabi, S.A. and Ogunmuyiwa, E., "Processing parameters influence on wear resistance behaviour of friction stir processed Al-TiC composites", ***Advances in Materials Science and Engineering***, Vol. 2014, (2014), 1-12, doi: 10.1155/2014/724590
17. Bauri, R., Yadav, D. and Suhas, G., "Effect of friction stir processing (FSP) on microstructure and properties of Al--TiC in situ composite", ***Materials Science and Engineering: A***, Vol. 528, No. 13, (2011), 4732-4739, doi: 10.1016/j.msea.2011.02.085.
18. Sharma, V., Gupta, Y., Kumar, B.M. and Prakash, U., "Friction Stir Processing Strategies for Uniform Distribution of Reinforcement in a Surface Composite", ***Materials and Manufacturing Processes***, Vol. 31, No. 10, (2016), 1384-1392, doi: 10.1080/10426914.2015.1103869.
19. Costa, J.D.M., Jesus, J.S., Loureiro, A., Ferreira, J.A.M. and Borrego, L.P., "Fatigue life improvement of mig welded aluminium T-joints by friction stir processing", ***International Journal of Fatigue***, Vol. 61, (2014), 244-254, doi: 10.1016/j.ijfatigue.2013.11.004.
20. Borrego, L.P., Costa, J.D., Jesus, J.S., Loureiro, A.R. and Ferreira, J.M., "Fatigue life improvement by friction stir processing of 5083 aluminium alloy MIG butt welds", ***Theoretical and Applied Fracture Mechanics***, Vol. 70, (2014) 68-74, doi: 10.1016/j.tafmec.2014.02.002.
21. Xu, N. and Bao, Y., "Enhanced mechanical properties of tungsten inert gas welded AZ31 magnesium alloy joint using two-pass friction stir processing with rapid cooling", ***Materials Science and Engineering: A***, Vol. 655, (2016), 292-299, doi: 10.1016/j.msea.2016.01.009.
22. S. Mabuwa and V. Msomi, "Friction Stir Processing Of TIG And Friction Stir Welded Dissimilar Alloy Joints: A Review", (2019), doi: 10.20944/preprints201910.0226.v1.
23. Abbasi, M., Givi, M. and Bagheri, B., "New method to enhance the mechanical characteristics of Al-5052 alloy weldment produced by tungsten inert gas", ***Proceedings of the Institution of Mechanical Engineers, Part B: Journal of Engineering Manufacture***, (2020), doi: 10.1177/0954405420929777.
24. Mehdi, H. and Mishra, R.S., "Effect of friction stir processing on mechanical properties and heat transfer of TIG welded joint of AA6061 and AA7075", ***Defence Technology***, Vol. 17, No. 3, (2020), 715-727, doi:10.1016/j.dt.2020.04.014.
25. Tandel, K.D. and Menghani, J.V., "Autogenous TIG Welding of Al-5083-H111 Butt Joint", ***In Advances in Manufacturing Processes***, (2021), 205-219, doi: 10.1007/978-981-15-9117-4_16.
26. Rezaei, G. and Arab, N. B. M. "Investigation on Tensile Strength of Friction Stir Welded Joints in PP/EPDM/Clay Nanocomposites", ***International Journal of Engineering Transactions C: Aspects***, Vol. 28, (2015), 1382-1391, doi: 10.5829/idosi.ije.2015.28.09c.17.
27. Zhao, H., Pan, Q., Qin, Q., Wu, Y. and Su, X., "Effect of the processing parameters of friction stir processing on the microstructure and mechanical properties of 6063 aluminum alloy", ***Materials Science and Engineering: A***, Vol. 751, (2019), 70-79, doi: 10.1016/j.msea.2019.02.064.
28. Hasanzadeh R. and Azdast, T., "Welding Properties of Polymeric Nanocomposite Parts Containing Alumina Nanoparticles in Friction Stir Welding Process", ***International Journal of Engineering Transactions A: Basics***, Vol. 30, (2017), 143-151, doi: 10.5829/idosi.ije.2017.30.01a.18.
29. Fuller, C.B. and Mahoney, M.W., "The effect of friction stir proce ssing on 5083-H321/5356 Al arc welds: Microstructural and mechanical analysis", ***Metallurgical and Materials Transactions A***, Vol. 37, No. 12, (2006), 3605-3615, doi:10.1007/s11661-006-1055-1.
30. Jiang, Z., Hua, X., Huang, L., Wu, D. and Li, F., "Effect of multiple thermal cycles on metallurgical and mechanical properties during multi-pass gas metal arc welding of Al 5083 alloy", ***The International Journal of Advanced Manufacturing Technology***, Vol. 93, No. 9-12, (2017), 3799-3811, doi: 10.1007/s00170-017-0771-6.
31. Chaurasia, P.K., Pandey, C., Giri, A., Saini, N. and Mahapatra, M.M., "A comparative study of residual stress and mechanical properties for FSW and TIG weld on structural steel", ***Archives of Metallurgy and Materials***, Vol. 63, (2017), 1019-1029, doi: 10.24425/122437.
32. Węglowski, M.S., "Friction stir processing -- State of the art", ***Archives of civil and Mechanical Engineering***, Vol. 18, No. 1, (2018), 114-129, doi: 10.1016/j.acme.2017.06.002.

Persian Abstract

چکیده

جوشکاری با گاز خنثی تنگستن (TIG)ترجیح داده شده ترین فرآیند اتصال برای آلیاژهای آلومینیوم است، اما به دلیل محدودیت های ذاتی فرآیند، اتصال جوشی را تولید می کند که دارای خواص مکانیکی پایین تری در مقایسه با فلز پایه است. برای بهبود خواص مکانیکی، جوش توسط پردازش اغتشاشی اصطکاکی (FSP)تا عمق ۲ میلی متر پس از پردازش می شود. این مقاله تاثیر اجرای FSP را بر روی اتصال لب به لب جوش داده شده خودبخود TIG صفحه Al-5083 با ضخامت ٦ میلی متر ارائه می دهد. خواص مکانیکی و متالورژیکی جوش TIG خودزای فرآوری شده و فرآوری نشده مقایسه شده است. تکنیک‌های مشخصه‌ای که برای ارزیابی اتصال جوش اتخاذ شده‌اند عبارتند از: تست کششی، اندازه‌گیری ریزسختی، بررسی‌های ریزساختاری و آنالیز .SEMاستحکام کششی اتصال جوش TIG 6.5 درصد نسبت به فلز پایه به دلیل وجود تخلخل های ریز در فلز جوش کاهش می یابد. پردازش اغتشاشی اصطکاکی ساختار تصفیه شده دانه ریز را تولید می کند، استحکام کششی اتصال جوش TIG خودزا را تا ۲.۷ درصد بهبود می بخشد. ریزسختی فلز جوش TIG خودزاد سطح از HV ١٦٣.٦ به HV ۲۹۸ پس از انجام FSP افزایش می یابد. با این حال، تصاویر SEM از سطح شکسته نمونه پردازش شده با اغتشاش اصطکاکی، ساختار فرورفتگی ظریفی را نشان می‌دهد که نشان می‌دهد شکل‌پذیری اتصال جوش پس از انجام FSP روی اتصال جوش TIG خودزا، بی‌تأثیر باقی می‌ماند.